Dynamic Light Scattering Study of Poly(*N*-isopropylacrylamide-*co*-acrylic acid) Gels

Mitsuhiro Shibayama,* Yoshihiro Fujikawa, and Shunji Nomura

Department of Polymer Science and Engineering, Kyoto Institute of Technology, Matsugasaki, Sakyo-ku, Kyoto 606, Japan

Received February 27, 1996; Revised Manuscript Received June 18, 1996[⊗]

ABSTRACT: Spatial inhomogeneities of poly(*N*-isopropylacrylamide-*co*-acrylic acid) (NIPA/AAc) gels were investigated by dynamic light scattering as a function of AAc comonomer concentration and temperature. The results showed the following: (1) The ensemble average scattered intensity, $\langle I \rangle_E$, decreased with increasing AAc comonomer concentration and increased with temperature. (2) Dynamic fluctuations increased with temperature and diverged at the transition temperature, T_c. (3) Above the Θ temperature of NIPA homopolymer in an aqueous solution, the intensity−intensity time correlation function did not fit a single-exponential function, but fit a double exponential or a stretched exponential, indicating a heterogeneous structure, i.e., polymer-rich and polymer-poor phases at temperatures above Θ.

Introduction

Poly(*N*-isopropylacrylamide) (PNIPA) is a model system for studying hydrophobic interactions. As extensively reviewed by Shild,[1] the number of studies of PNIPA has increased sharply in recent years. PNIPA undergoes a coil-to-globule transition around 32 °C. In the case of the PNIPA gel, a volume phase transition takes place on increasing the temperature around 33.8 °C (≈Θ).[2] Though this transition is continuous, the transition becomes discontinuous in gels containing a small amount of a chargeable comonomer, e.g., acrylic acid (AAc).[3] The discrete transition observed in poly(NIPA/AAc) gels is explained with conventional theories on gel swelling, in which the Donnan potential (or free energy of the counterions) leads to swelling and the elastic energy of the network chains keeps a finite size of the gel with the aid of the mixing energy of the network with the solvent.

The microscopic views of the volume transition have been extensively studied by various methods, including dynamic light scattering,[4] NMR,[5] small-angle neutron scattering (SANS),[6−8] fluorescence spectroscopy,[9] and infrared absorption spectroscopy.[11] Shibayama et al. reported that a microphase separation takes place in a weakly charged poly(NIPA/AAc) gel before a macroscopic discrete volume phase transition takes place during heating.[7,8] This observation is consistent with the prediction by Borue and Erukhimovich, of a microphase-separated structure in polyelectrolyte solutions in a poor solvent.[11] SANS studies were used to investigate the pH and salt concentration dependence of the microscopic structures of NIPA/AAc gels.[12] Thermal analysis also proved the existence of the microphase separation at a lower temperature than the macroscopic volume transition temperature.[13]

On the basis of these recent developments of the understanding of the relation between the hydrophobic interactions and microscopic structures of NIPA/AAc gels, we report here the dynamic aspects of NIPA/AAc copolymer gels by dynamic light scattering (DLS). DLS is a useful tool to investigate the nature of gels which consist of dynamic fluctuations superimposed on the static inhomogeneities inherent in the network. The objectives of this paper are to investigate the comonomer (AAc) concentration and temperature dependence of the structure and heterogeneity parameters, such as the correlation length, ξ, and the scattered intensities of the dynamic and static parts.

Table 1. Sample Codes and Compositions

	concentrations at preparation	
code	AAc (mM)	NIPA (mM)
0 mM	0	700
4 mM	4	696
8 mM	8	692
12 mM	12	688
16 mM	16	684
32 mM	32	668

Experimental Section

Samples. Prescribed amounts of recrystallized *N*-isopropylacrylamide (NIPA) (Kohjin Chemical Co. Ltd.) and acrylic acid (AAc) (Wako Chemical Co.) were dissolved in deionized water. The total concentration of NIPA and AAc was kept constant (700 mM), while the AAc monomer concentration was varied from 0 to 4, 8, 12, 16, and 32 mM. *N*,*N*′-Methylenebisacrylamide (BIS) (8.6 mM) and ammonium persulfate (APS) (1.88 mM) were added to the solutions, this pregel solution was degassed, and polymerization was initiated in a 10-mm-diameter test tube by *N*,*N*,*N*′,*N*′-tetramethylethylenediamine (TEMED) (32 mM) at 20 °C for 20 h. Thus gel samples were used for DLS experiments without further treatment. Table 1 shows the sample codes and their compositions.

Dynamic Light Scattering. Dynamic light scattering experiments used a DLS instrument, consisting of a 5 mW He−Ne laser and laboratory-made optics. The sample tube was immersed in a refractive-index-matched silicone bath, thermostated within ±0.1 °C. When temperature was varied, 10 days was allowed for gel equilibration. The photon correlation was taken with a DLS-7 correlator (equivalent to a DLS-7000, Otsuka Electric Co.). The channel number of the time axis was 1024 and the so-called time interval photon correlation mode was employed. Sampling times of 1, 4, 8, and 20 μs were chosen, according to the relaxation rate of the gel. The correlation curve was accumulated 100 times to eliminate noise, followed by data acquisition at different sample positions by rotating the sample tube either 50 or 100 times for ensemble averaging. The scattering angle was fixed at 60°.

Theoretical Background

For an ergodic medium, the intensity−intensity time correlation function, $C_T(q,\tau)$, is given by

* To whom correspondence should be addressed.

[⊗] Abstract published in *Advance ACS Abstracts,* September 1, 1996.

S0024-9297(96)00320-8 CCC: $12.00

$$C_T(q,\tau) \equiv \frac{\langle I(q,0)I^*(q,\tau)\rangle_T}{\langle |I(q,0)|^2\rangle_T} = 1 + \alpha|g^{(1)}(q,\tau)|^2 \quad (1)$$

where q is the magnitude of the scattering vector, τ is the time difference between the photons, $I(q,\tau)$ is the scattered intensity at q and τ, and $I^*(q,\tau)$ is the complex conjugate of $I(q,\tau)$, respectively. $\langle\ \rangle_T$ denotes the time average and α ($0 < \alpha < 1$) is the instrumental coherence factor. In the case of our experimental setup, α is estimated to be 0.8. $g^{(1)}(q,\tau)$ is the scattering field correlation function,

$$g^{(1)}(q,\tau) = \exp[-Dq^2\tau] \quad (2)$$

where D is the diffusion coefficient. In the case of polymer gels swollen in a solvent, D is regarded as the cooperative diffusion coefficient characterizing the dynamics of the network chains and a single-exponential intensity time correlation function is observed.[14] In order to apply the theory to a DLS analysis of gels, however, the nonergodicity of gels has to be taken into account.[15,16] Thus the correlation function is given by[17]

$$C_T(q,\tau) = 1 + \alpha\sigma_I^2 \exp[-2D_A q^2\tau] + \epsilon \quad (3)$$

where σ_I^2 is the coherence factor ($0 < \sigma_I^2 < 1$) and ϵ ($\approx$0) is the time-independent background in this time scale. D_A is the apparent diffusion coefficient obtained at a given sample position and varies with the sample position in the range D (pure heterodyne) $\leq 2D_A \leq 2D$ (pure homodyne). The coherence factor σ_I^2 is related to the ratio, X, of the fluctuating (dynamic) component of the time average of the scattered intensity, $\langle I_F\rangle_T$, with respect to the total time average scattered intensity, $\langle I\rangle_T$, with

$$X \equiv \frac{\langle I_F\rangle_T}{\langle I\rangle_T} = 1 - (1 - \sigma_I^2)^{1/2} \quad (4)$$

$$D_A = D/(2 - X) = \frac{D}{2 - \langle I_F\rangle_T/\langle I\rangle_T} \quad (5)$$

D_A and $\langle I\rangle_T$ are observable quantities. Therefore, by plotting D_A as a function of $\langle I\rangle_T$, D and $\langle I_F\rangle_T$ can be estimated by curve fitting with eq 5. This method is called the partial heterodyne analysis, proposed by Joosten et al.[18] Equation 5 can be written in the following form:

$$\frac{\langle I\rangle_T}{D_A} = \frac{2}{D}\langle I\rangle_T - \frac{\langle I_F\rangle_T}{D} \quad (5a)$$

Hence, we propose the plot, $\langle I\rangle_T/D_A$ vs $\langle I\rangle_T$, because $\langle I\rangle_T/D_A$ is a linear function of $\langle I\rangle_T$, and D and $\langle I_F\rangle_T$ can be obtained from the slope and intercept.

If the gel consists of two phases, such as polymer-rich and polymer-poor phases, $C_T(q,\tau)$ is modified to

$$C_T(q,\tau) = 1 + A_1 \exp[-2D_1q^2\tau] + A_2 \exp[-2D_2q^2\tau] + \epsilon \quad (6)$$

where A_1 and A_2 are the intensities of the dynamic fluctuations and D_1 and D_2 are the diffusion coefficients of the individual phases, respectively. Equation 6 is expected for microphase-separated gels. A double-exponential decay is also observed for a system having a local oscillator. In this case, however, D_1 and D_2 are highly related to each other, i.e., $D_1 = 2D_2 = D$, because D_1 and D_2 represent homodyne and heterodyne terms, respectively.[16] It is reported that a nonexponential relaxation phenomenon is usually observed in the vicinity of the sol−gel transition and/or glass transition.[19,20] In order to describe this nonexponential relaxation, a stretched exponential function proposed by Kohlrausch[21] and Williams and Watts (KWW)[22] is commonly employed,

$$C_T(\tau) = C_1 + C_2 \exp[-(\tau/\tau_s)^\beta] \quad (7)$$

where C_1 and C_2 are constants and β and τ_s are the stretched exponent and the characteristic relaxation time, respectively. In the case of NIPA/AAc gels employed in this work, the dynamics of the concentration fluctuations changes dramatically in the vicinity of the volume transition temperature. Thus, the applicability of each of the correlation functions listed above will be examined.

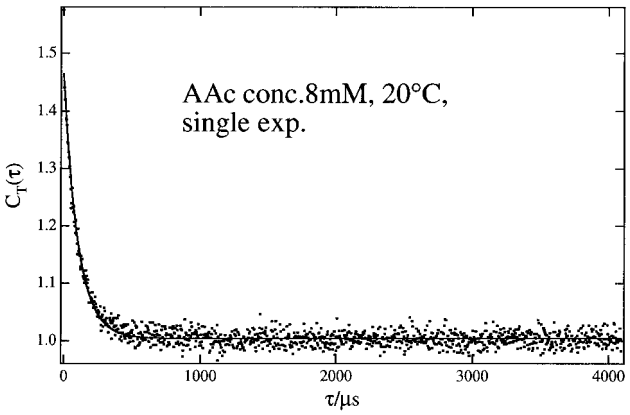

Figure 1. Time average intensity−intensity time correlation function, $C_T(t)$, for 8 mM gel (NIPA/AAc = 692/8) observed at 20 °C.

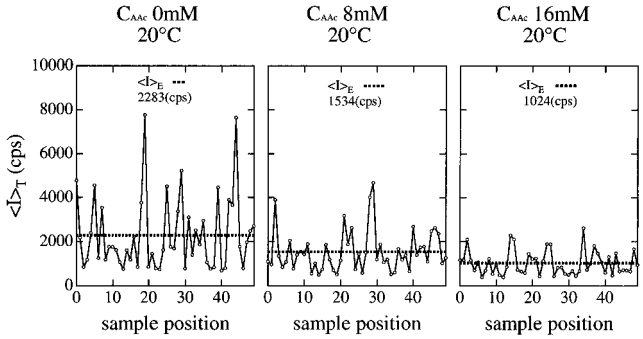

Figure 2. AAc content dependence of scattered intensity variation with sample position. $\langle I\rangle_T$ denotes the time average of the scattered intensity.

Results and Discussion

1. Static Inhomogeneities. Figure 1 shows the time correlation function $C_T(\tau)$ for NIPA/AAc gel containing 8 mM AAc (8 mM gel) at 20 °C. As shown in the figure, the observed data points (dots) are well fitted with a single-exponential function (eq 3). The evaluated apparent diffusion coefficient D_A is $(2.7 \pm 0.1) \times 10^{-7}$ cm^2/s, the coherence factor σ_I^2 is 0.46 ± 0.01, and ϵ is 0.0043 ± 0.0001. Note that D_A is the same order as for NIPA homopolymer gels in water at 20 °C.[23]

Figure 2 shows the speckle patterns of 0 mM, 8 mM, and 16 mM gels at 20 °C. Fifty different positions of the sample were arbitrarily chosen, and the scattered

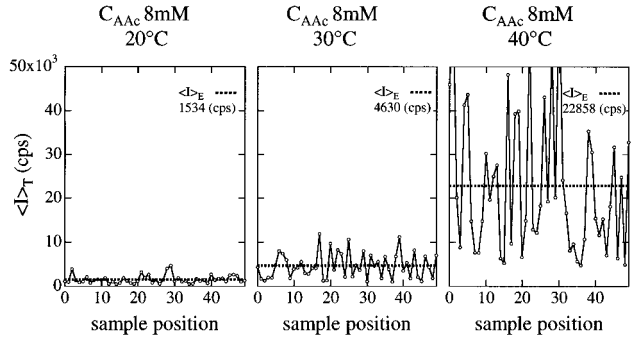

Figure 3. Temperature dependence of scattered intensity variation with sample position. $\langle I\rangle_T$ denotes the time average of the scattered intensity.

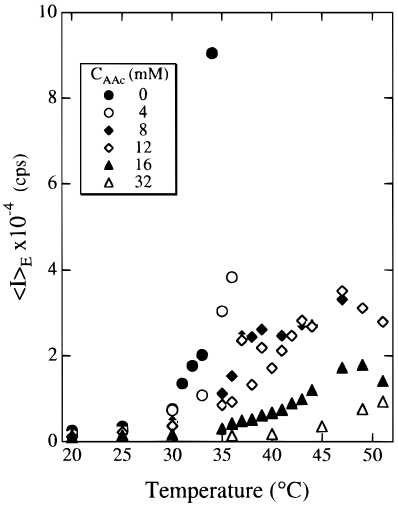

Figure 4. Temperature dependence of the ensemble average scattered intensity, $\langle I\rangle_E$ for gels having different AAc contents.

intensity was observed at each position. The time average scattered intensity, $\langle I\rangle_T$, varies randomly with the sample position. The dotted lines in the figures indicate the ensemble average of the time average scattered intensity, $\langle I\rangle_E$. Note that the sampling number of 50 is definitely too small to obtain an ensemble average. Therefore we conduct a qualitative analysis for $\langle I\rangle_E$. It is clear that $\langle I\rangle_E$ decreases with increasing C_{AAc}. This indicates that the spatial inhomogeneities are significantly suppressed by the AAc residues in the network. This is due to an increase in the osmotic pressure of the network, resulting from the Donnan potential of the charged AAc groups. The increase of the osmotic pressure leads to an increase in the bulk modulus of the gel (or a decrease in the osmotic compressibility), resulting in the suppression of the concentration fluctuations.

When the temperature is raised, the Donnan potential has to compete against the deswelling power of the NIPA network because of hydrophobic bonding of NIPA residues at a temperature above the so-called Θ temperature of NIPA homopolymer gels (≈33.8 °C).[7] Figure 3 shows the speckle patterns of 8 mM gel at 20, 30, and 40 °C. As shown in the figures, $\langle I\rangle_E$ increases with temperature. Particularly, at 40 °C (>Θ), a strong speckle pattern is observed. Note that $\langle I\rangle_E$ at 40 °C is about 5 times larger than that at 30 °C.

Figure 4 summarizes the temperature dependence of $\langle I\rangle_E$ for gels having different C_{AAc}'s. For each gel, $\langle I\rangle_E$ starts to increase above 30 °C. However, the rise of $\langle I\rangle_E$ is C_{AAc} dependent. The lower C_{AAc}, the higher is $\langle I\rangle_E$. This again indicates that addition of AAc residues to the NIPA network leads to a suppression of spatial inhomogeneities. Another feature is the decrease of $\langle I\rangle_E$ in 12 and 16 mM gels above 45 and 47 °C, respectively. This may indicate that a relaxation to an equilibrium structure in the shrunken state takes place. Such a reorganization of the structure may be allowed only in the case where the mobility of the network is sufficient.

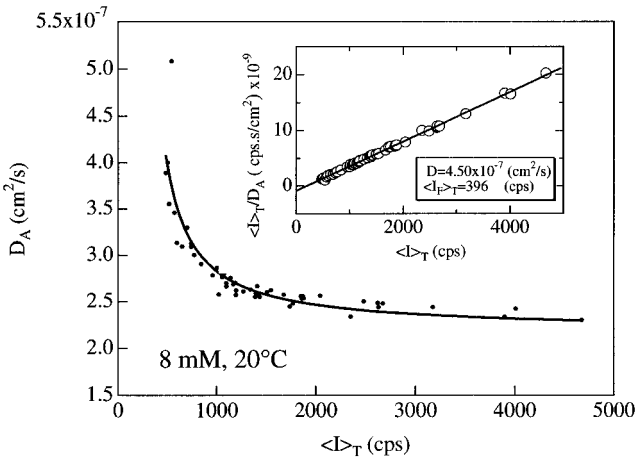

Figure 5. Plot of D_A as a function of $\langle I\rangle_T$ for 8 mM gel at 20 °C. The data points were fitted with eq 5. The fitted curve is shown with the solid line. The inset shows the $\langle I\rangle_T/D_A$ vs $\langle I\rangle_T$ plot, from which D and $\langle I_F\rangle_T$ are estimated by using eq 5a. The values of D and $\langle I_F\rangle_T$ estimated by these plots agree with each other.

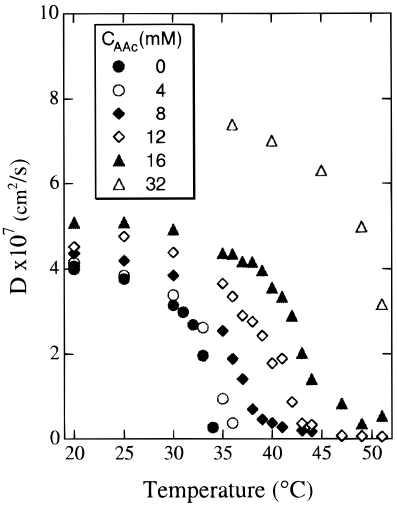

Figure 6. Temperature dependence of the diffusion coefficient, D, for gels with different AAc contents.

2. Dynamic Fluctuations. Figure 5 shows D_A as a function of $\langle I\rangle_T$ for 8 mM gel at 20 °C. The solid curve is drawn by curve fitting with eq 5, from which the diffusion coefficient D and the fluctuating component of the time average scattered intensity, $\langle I_F\rangle_T$, are estimated. The plot in the inset, $\langle I\rangle_T/D_A$ vs $\langle I\rangle$ plot, gives a straight line as predicted by eq 5a. Note that this plot gives D and $\langle I_F\rangle_T$ with higher precision although the number of data points is not sufficient for "ensemble average". D and $\langle I_F\rangle_T$ for other sets of data obtained at different temperatures and/or on different samples were estimated in the same manner.

Figure 6 shows the temperature dependence of the diffusion coefficient, D, for gels with different C_{AAc}'s. Note that since D is estimated by using eq 5a, it represents the dynamics of the gel irrespective of the sample position. Below 30 °C (≈Θ), D is rather invariant with temperature, but it drops steeply with increas-

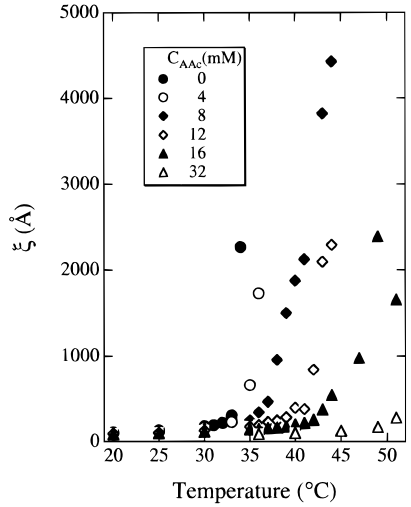

Figure 7. Temperature dependence of the correlation length, ξ, for gels with different AAc contents.

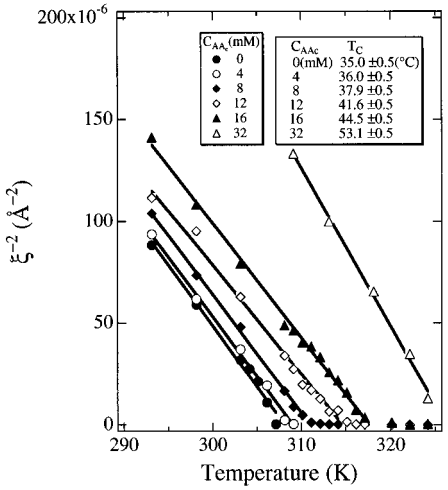

Figure 8. ξ^{-2} vs temperature plot. The transition temperatures, T_c's, obtained by extrapolating $\xi^{-2} = 0$ are listed in the inset.

ing temperature above Θ. This suggests that a critical slowing down of the cooperative diffusion takes place on approaching the critical temperature. A similar phenomenon was observed by Tanaka et al.[23] for NIPA homopolymer gels and Orkisz et al.[24] for NIPA/AAc gels.

The correlation length, ξ, is estimated from D by[25]

$$\xi = \frac{kT}{6\pi\eta D} \tag{8}$$

where kT is the Boltzmann energy and η is the solvent viscosity. Figure 7 shows the temperature dependence of the correlation length, ξ, for gels having different C_{AAc}'s. This figure clearly shows that ξ diverges with increasing temperature. The critical temperature is estimated in the context of the mean field assumption, i.e., ξ^{-2} vs T plot. Figure 8 shows the variation of ξ^{-2} as a function of temperature. As shown in the figure, ξ^{-2} decreases rather linearly with T. The critical temperatures, T_c's, at which the correlation length diverges, are obtained at the intercept of the T axis and are listed in the inset. Though the values of T_c will be discussed later in conjunction with those obtained by other methods, the higher the C_{AAc}, the higher is T_c.

3. Critical and Two-Phase Fluctuations. Above Θ, a single-exponential fit of $C_T(\tau)$ is unsatisfactory as

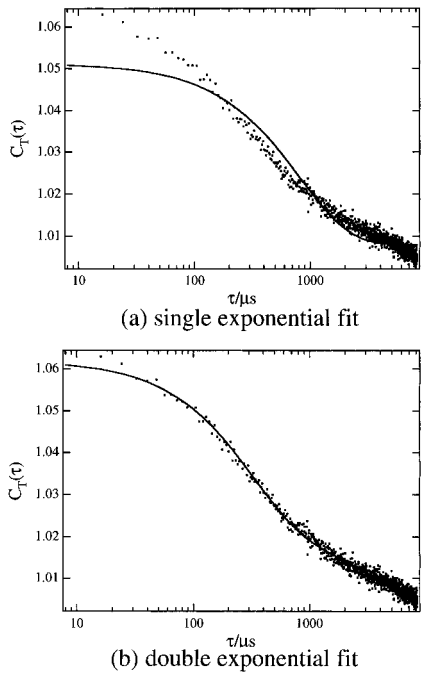

Figure 9. Time average intensity−intensity time correlation function, $C_T(t)$, for 8 mM gel (NIPA/AAc = 692/8) observed at 38 °C and the results of the curve fittings with (a) a single-exponential and (b) a double-exponential function. Note that the time axis is taken in logarithmic scale so as to emphasize the deviation.

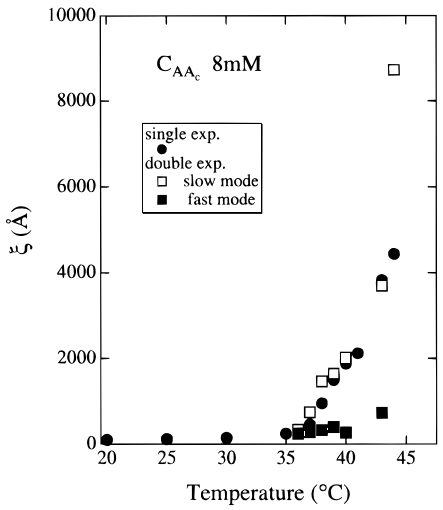

Figure 10. Temperature dependence of ξ estimated with the single- and the double-exponential fits.

shown in Figure 9a. This is due mainly to an appearance of microphase separation as reported by Shibayama et al.[7,8] An example of a double-exponential fit is shown in Figure 9b, for an 8 mM gel at 38 °C. In this case, two different diffusion coefficients can be evaluated by the partial heterodyne analysis, from which two different correlation lengths are obtained by using eq 8. Figure 10 shows the temperature dependence of the correlation length, ξ, for an 8 mM gel. Above 35 °C, there are two ξ's, one for the fast mode and the other for the slow mode. Note that no simple relation exists between ξ_{fast} and ξ_{slow}. If the system is homogeneous but having a local oscillator, the relation $\xi_{slow} = 2\xi_{fast}$ is expected because of D_{fast} ($=D_{homodyne}$) = $2D_{slow}$ ($=2D_{heterodyne}$). Therefore, the presence of two characteristic relaxation process indicates two phases. It is also noteworthy that ξ for the slow mode (at $T >$

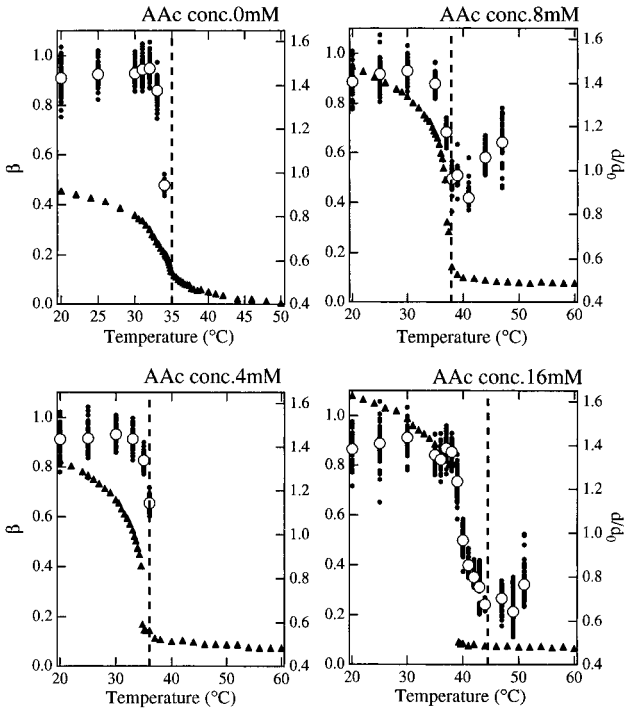

Figure 11. Temperature dependence of the stretched exponential, β, for gels having different AAc contents.

35 °C), ξ_{slow}, is very close to the one estimated with the single-exponential fit. Therefore, the ξ_{slow} corresponds to the new phase, i.e., the collapsed phase (i.e., the hydrophobic phase). On the other hand, ξ_{fast} is on the same order as ξ at $T < \Theta$, indicating that ξ_{fast} is related to the water-rich phase, i.e., the hydrophilic phase around the charged AAc groups. The following point should be noted here. The phase discussed here is not the same as the phase having a sharp boundary. The former is analogous to the phase of polymer blends with a diffuse boundary (weak segregation limit).

As discussed in the Theoretical Background section, another method to describe a non-single-exponential decay function is the KWW stretched exponential function. A curve fitting of $C_T(\tau)$ with the stretched function (eq 7) was also successful. Figure 11 shows the temperature dependence of the stretched exponential fit parameter, β (dots and open circles), as well as the shrinking curve of the gel, d/d_0 (solid triangles), for (a) 0 mM gel, (b) 4 mM gel, (c) 8 mM gel, and (d) 16 mM gel, where d and d_0 are the gel diameters at the given temperature and at preparation, respectively. The dashed vertical lines indicate the critical temperature obtained by the ξ^{-2} vs T plot (Figure 8). The dots indicate the individual values of β for each fit of the correlation functions obtained at different positions, and the open circle is their average. Here β is close to unity for T far below T_c. This supports the validity of the single-exponential fit at low temperatures. However, β decreases on approaching T_c. Orkisz discussed this phenomenon by using a power law function assuming a fractal nature of the object.[24] However, in the case of NIPA/AAc gels at an elevated temperature, this kind of argument is unconvincing because it is clear by SANS analysis that two phases coexist. Thus, we believe that the deviation of β from unity is due to the appearance of two phases. Another interesting aspect in the temperature variation of β is the upturn of β above T_c, which is observed for 8 and 16 mM gels. This phenomenon

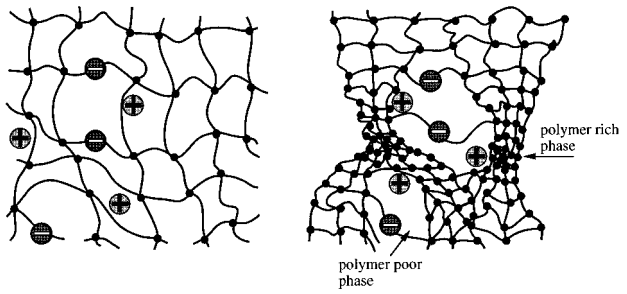

Figure 12. Schematic representation of the network in (a) the one-state phase (at $T < \Theta$) and (b) the two-phase state (at $T > \Theta$).

was observed by Furukawa and Hirotsu for NIPA homopolymer gels.[26] They found gels to become homogeneous at $T \gg T_c$ when the temperature was varied very slowly, ensuring thermal equilibrium at each temperature. This may be the reason for the upturn of β. In our case, such a behavior was not observed for 0 and 4 mM gels because the structure of these gels may have been frozen-in at $T > T_c$. The upturn behavior of β for 12 mM and 16 mM gels is consistent with the decrease in $\langle I \rangle_E$ for these gels at high temperatures as discussed in Figure 4.

Figure 12 shows models of the NIPA/AAc gels at low ($T < \Theta$) and high temperatures ($T > \Theta$). At low temperatures, the gel network is more or less homogeneous, giving rise to a unique value of the diffusion coefficient, D. Note that in comparison with D, D_A varies with position even at these temperatures, due to the nonergodicity (or spatial inhomogeneity) resulting from the nature of the network. Thus the variation of D_A has nothing to do with the inhomogeneity of the network in a sense of the dynamic fluctuations. However, at $T > \Theta$, the gel network becomes heterogeneous and polymer-rich and -poor phases are created due to the antagonistic interactions between hydrophobic (polymer rich) and hydrophilic (polymer poor) interactions. This is why the double exponential or the stretched exponential function describes well the observed time correlation function. A shrinking transition takes place at T_c, which is above Θ if AAc comonomers are present in the NIPA network.

4. Transition Temperature. In the preceding sections, we discuss the transition temperature, T_c, as the temperature at which the correlation length diverges. In the literature, however, T_c of gels undergoing volume transition is defined from different aspects.[2−11,13,26] For example, T_c determined by swelling−shrinking curve corresponds to the temperature at which a volume transition takes place. For noncharged gels, this temperature is consistent with that at $\xi \rightarrow \infty$. However, in the case of charged gels, the physical meaning of T_c is not well interpreted because of formation of heterophases, i.e., polymer-rich and -poor phases. Therefore, it is of importance to compare the T_c's observed by different methods. Figure 13 shows the C_{AAc} dependence of the transition temperatures measured by (a) the shrinking curve,[13] (b) DSC,[13] and (c) DLS (this work). The T_c obtained by DSC corresponds to the onset of microphase separation because the detected endotherm is related to the hydrophobic bonding. This is highly affected by the change of local environment of NIPA chains in a solvent. Since NIPA chains start to shrink in the presence of water at Θ, it is reasonable that the T_c obtained by DSC is close to

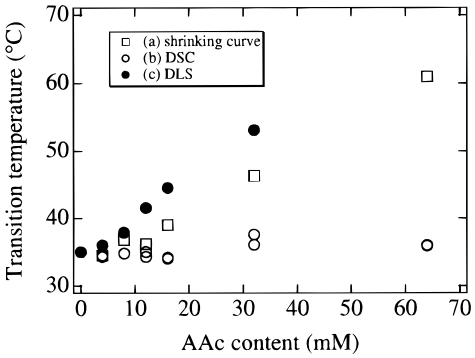

Figure 13. AAc content dependence of the transition temperatures evaluated by (a) the shrinking curve measurement, (b) DSC, and (c) DLS.

the onset of the microphase separation. Contrary to this, the T_c by the shrinking curve measurement is the temperature at which a "macroscopic" volume transition takes place, which is a result of the competition between the tendency of NIPA chains to shrink (the hydrophobic association interaction) and the tendency of the AAc residues to expand (the Donnan potential). For charged gels, therefore, the T_c by shrinking measurement is higher than that by DSC because the hydrophobic interaction has to be stronger that the Donnan potential and such situation is fulfilled by increasing temperature. Refer to ref 13 for further discussions. Regarding T_c by DLS, we expect a good agreement with that by volumetric analysis (shrinking curve measurement). However, Figure 13 shows that the T_c obtained by DLS is even higher than that by shrinking curve. This may be partially due to the single-exponential analysis for the determination of T_c. For example, Figure 10 indicates that ξ of the slow mode by double-exponential fit diverges at a lower temperature than that by single-exponential analysis. Although a further analysis was tried, the double-exponential analysis became less reliable for the gels with higher C_{AAc}'s due to lower scattered intensity. Therefore, we reserve this problem as a future work.

Concluding Remarks

The static and dynamic fluctuations of poly(*N*-isopropylacrylamide-*co*-acrylic acid) (NIPA/AAc) copolymer gels were investigated with dynamic light scattering. The static fluctuations, investigated with the ensemble average of the scattered intensity, $\langle I \rangle_E$, decreased with increasing AAc content, whereas they increased with temperature. The correlation length, ξ, a spatial measure of the dynamic fluctuations, is also a strong function of AAc content. The role of AAc comonomers in the gel is explained as a fluctuation reducing agent, which comes from a generation of a strong osmotic pressure by ionization of the AAc group. At a temperature above the Θ temperature of NIPA homopolymer gels, this osmotic stabilization has to compete against the strong hydrophobic bonding of the NIPA main chain network. Thus, both static and dynamic fluctuations increased with temperature and ξ diverged at the critical temperature, T_c ($\geq\Theta$).

Above Θ, the intensity−intensity time correlation function, $C_T(\tau)$, was described with either a double-exponential function or a stretched exponential function. This indicates an appearance of two phases, a hydrophobic polymer-rich and a hydrophilic polymer-poor phase. The stretched exponent, β, remained constant at $T \ll \Theta$, decreased steeply at T_c, and recovered at higher temperatures.

Acknowledgment. This work is supported by the Ministry of Education, Science, Sports and Culture, Japan (Grant-in-Aid Nos. 07241242 and 08231245 to M.S.).

References and Notes

(1) Schild, H. G. *Prog. Polym. Sci.*, **1992**, *17*, 163.
(2) Hirokawa, Y.; Tanaka, T.; Matsuo, E. S. *J. Chem. Phys.* **1984**, *81*, 6379.
(3) Hirotsu, S.; Hirokawa, Y.; Tanaka, T. *J. Chem. Phys.* **1987**, *87*, 1392.
(4) Tanaka, T.; Ishiwata, S.; Ishimoto, C. *Phys. Rev. Lett.* **1977**, *38*, 771.
(5) Tokuhiro, T.; Amiya, T.; Mamada, A.; Tanaka, T. *Macromolecules* **1991**, *24*, 2936.
(6) Shibayama, M.; Tanaka, T.; Han, C. C. *J. Chem. Phys.* **1992**, *97*, 6829.
(7) Shibayama, M.; Tanaka, T.; Han, C. C. *J. Chem. Phys.* **1992**, *97*, 6842.
(8) Shibayama, M.; Tanaka, T. *J. Chem. Phys.* **1995**, *102*, 9392.
(9) Hu, Y.; Horie, K.; Ushiki, H. *Macromolecules* **1992**, *25*, 6040.
(10) Shibayama, M.; Morimoto, M.; Nomura, S. *Macromolecules* **1994**, *27*, 5060.
(11) Borue, V.; Erukhimovich, I. *Macromolecules* **1988**, *21*, 3240.
(12) Shibayama, M.; Ikkai, F.; Inamoto, S.; Nomura, S. *J. Chem. Phys.*, in press.
(13) Shibayama, M.; Mizutani, S.; Nomura, S. *Macromolecules* **1996**, *29*, 2019.
(14) Tanaka, T.; Hocker, L. O.; Benedek, G. B. *J. Chem. Phys.* **1973**, *59*, 5151.
(15) Pusey, P. N.; van Megen, W. *Physica A* **1989**, *157*, 705.
(16) Chu, B. *Laser Light Scattering*, 2nd ed.; Academic Press: San Diego, 1991.
(17) Shibayama, M.; Takeuchi, T.; Nomura, S. *Macromolecules* **1994**, *27*, 5350.
(18) Joosten, J. G. H.; McCarthy, J. L.; Pusey, P. N. *Macromolecules* **1991**, *24*, 6690.
(19) Martin, J. E.; Wilcoxon, J.; Odinek, J. *Phys. Rev. A* **1991**, *A43*, 858.
(20) Fang, L.; Brown, W.; Konak, C. *Macromolecules* **1991**, *24*, 6839.
(21) Kohlrausch, R. *Pogg. Ann. Phys.* **1854**, *91*, 179.
(22) Williams, G.; Watts, D. C. *Trans. Faraday Soc.* **1970**, *66*, 80.
(23) Tanaka, T.; Sato, E.; Hirokawa, Y.; Hirotsu, S.; Peetermans, J. *Phys. Rev. Lett.* **1985**, *55*, 2455.
(24) Orkisz, M. Ph.D. Dissertation, Physics Department, MIT, 1994.
(25) de Gennes, P.-G. *Scaling Concepts in Polymer Physics*; Cornell University Press: Ithaca, NY, 1978.
(26) Furukawa, H.; Hirotsu, S. *Polym. Prep. Jpn.*, **1995**, *44*, 1630.

MA960320W